

Anatomy Driven Deformation

D Gering¹, W Lu¹, K Ruchala¹, G Olivera^{1,2}

¹TomoTherapy Inc, Madison, WI, USA. ²Department of Medical Physics, University of Wisconsin, Madison, WI, USA.

Abstract

A new method of image deformation is proposed with the intent of improving the anatomical significance of the results. Instead of allowing each image voxel to move in any direction, only a few anatomical motions are permissible. The planning image and daily image are both segmented automatically. These segmentations are then analyzed to divine the values of the few parameters that govern the allowable motions. Given these model parameters, a deformation field is generated directly without iteration. This field is then passed into a pure free-form deformation process in order to account for any motion not captured by the model. Using a model to initially constrain the deformation field can help to mitigate errors.

Keywords

Image deformation, image segmentation, adaptive therapy

Introduction

Adaptive radiation therapy benefits from quantitative measures such as composite dose maps and dose volume histograms. The computation of these measures is enabled by a deformation process that warps the planning image to images acquired daily throughout the treatment regimen. Deformation methods have typically been based on optical flow, which implies that voxel brightness is considered without regard to the tissue type represented. The type of transformation discovered by the deformation method has typically been free-form, which allows each image voxel to move in all directions under a constraint of spatial smoothness.

A new method of anatomically driven deformation is proposed with the intent of improving the anatomical significance of the results. Instead of allowing each image voxel to move in any direction, only a few anatomical motions are permissible.

Material and methods

The planning image and daily image are both segmented automatically to label each voxel according to the tissue type represented: air, fat, muscle, and bone. This tissue segmentation lays the foundation for an automatic organ segmentation. The differences between the organ segmentations are analyzed to observe the motions of a few primary actors – cranium, spine, mandible, pharynx, and skin. These effects are integrated into a single warp field (Figure 2), which is an image that expresses a motion vector at every voxel location. Unlike typical deformation algorithms, the method is direct without

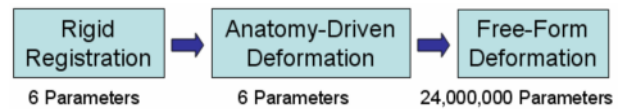


Figure 1: Similar to rigid registration, anatomy-driven deformation can be expressed with a handful of parameters, and it is useful for initializing free-form deformation.

iteration. This field is then passed into a pure free-form deformation process [3] in order to account for any motion not captured by the model.

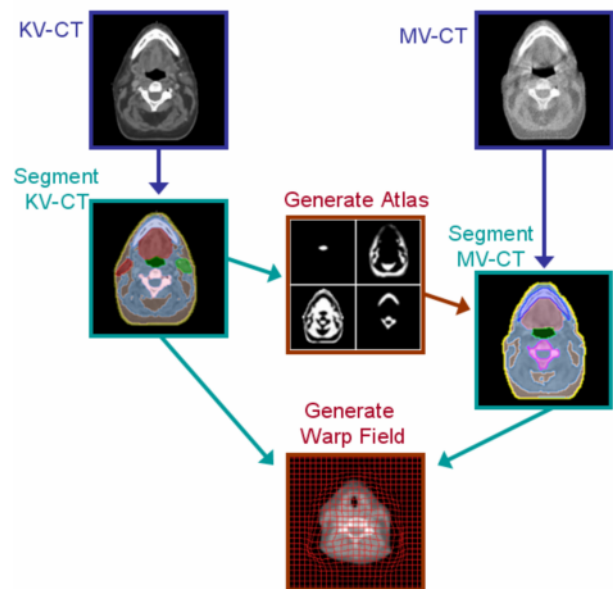


Figure 2: The segmentation of the high-quality planning image is used to guide the segmentation of the daily image.

Image Segmentation

A segmentation method using a five-layer hierarchy, proposed in [1,2], propagates information from the voxel layer up to voxel neighborhoods, then tissues, then organs, and finally organ systems.

Shape models composed of geometric primitives regularize the segmentations, as shown in Figure 3. Anatomic landmarks are relied upon for generating an expected region for an organ, and then the organ is roughly segmented. The shape model is fit to this draft segmentation, and then a final segmentation is performed where a strict threshold is applied outside the shape, and a loose threshold is employed inside the shape. This approach balances the strength of location information against the strength of CT signal information.

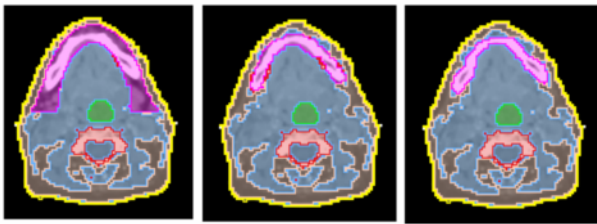


Figure 3: Consider the mandible colored in purple. From left to right are depicted the following: expected region based on anatomic landmarks, shape model expressed as an elliptic arch, and the final segmentation.

Daily images often feature a different contrast method, resolution, and signal-to-noise ratio than the high-quality planning image. Therefore, the segmentation of

the planning image is leveraged to generate a probabilistic atlas (spatially varying map of tissue probabilities) to assist in the segmentation of the daily image, as shown in Figure 4.

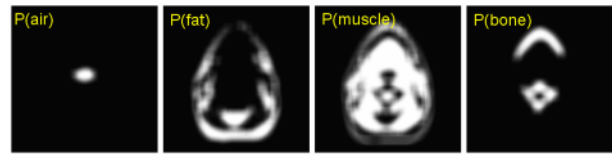


Figure 4: The KV-CT organ segmentation is converted into a tissue segmentation (only air, fat, muscle, and bone), which is then converted into a fuzzy probability map for use by the adaptive Bayesian classifier that segments the MV-CT image. In this figure, the brighter the voxel's intensity value, the more likely the tissue can be found there.

Deformation attributed to Bone Motions

The cranium, mandible, and spine are permitted to twist and shift as somewhat independent rigid bodies whose motions are governed by only four parameters. All four of these bone motions are depicted graphically in Figures 5-8. For example, the mandible expresses a swinging motion by rotating about the axis connecting its lateral "hinges" located superiorly and posteriorly.

Entirely independent from the mandible, the cranium and spine coordinate to perform 3 motions, as illustrated in Figures 6-8. The dens bone acts as the center of rotation for head tilt side-to-side, head nodding back-and-forth, and head swivel side-to-side. In our model, 80% of the rotation is attributed to C1, and the remainder is distributed across C2-C7 by interpolation.

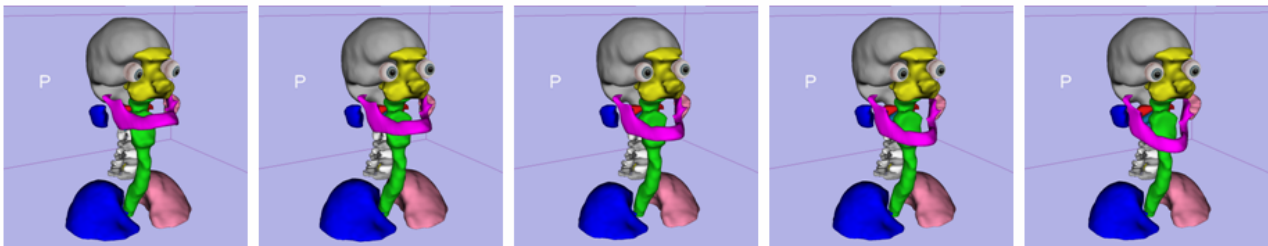


Figure 5: As we vary the single parameter that controls the mandible, it appears to swing up and down. The 3D surfaces are constructed from the automatic segmentation of the trachea (green), sinus (yellow), lungs (blue and pink), parotid glands (blue and pink) spine (gray and white), C1 (red), C2 (blue), brain (gray), and eyes (photo-realistic).

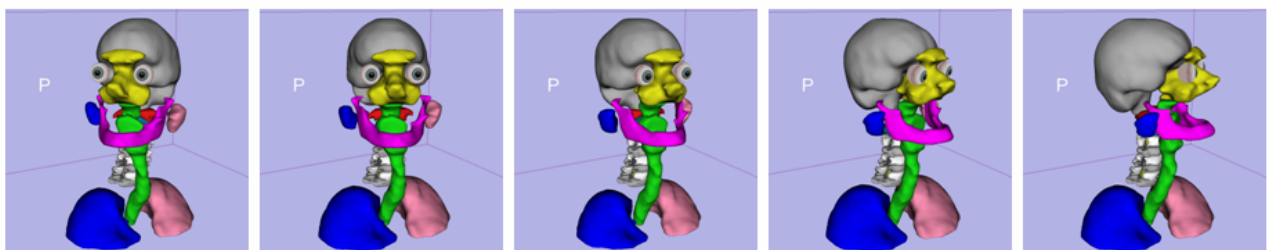


Figure 6: Head swivel, from side to side.

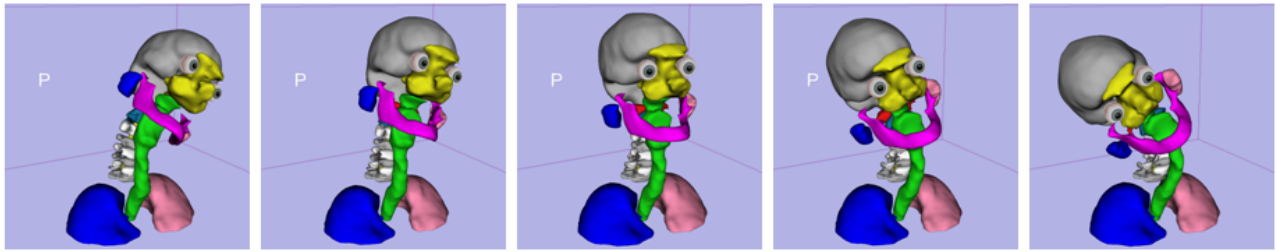


Figure 7: Head tilt, from side to side.

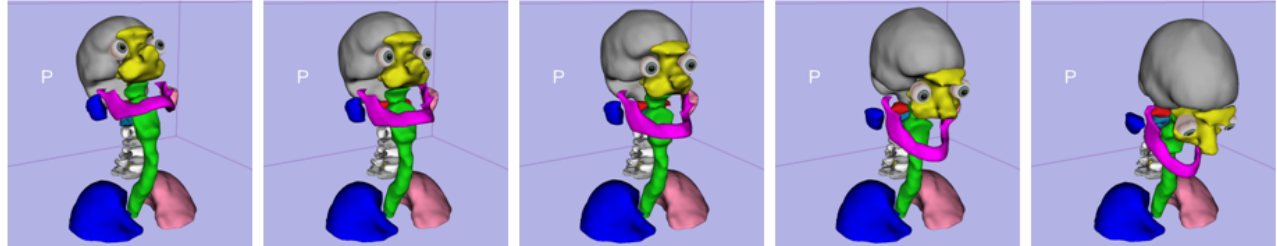


Figure 8: Head nodding, back and forth.

Deformation attributed to Weight Loss

All deviations between the two skin surfaces are attributed to weight loss. The difference is therefore reconciled by expanding the fatty tissue outward in a radial fashion in the axial plane. The origin of the radial expansion is the centroid of the spinal cord. On slices where the mandible is present, a central axis is drawn through the spine and mandible, as shown in Figure 9. The motion vectors are defined to emanate outward

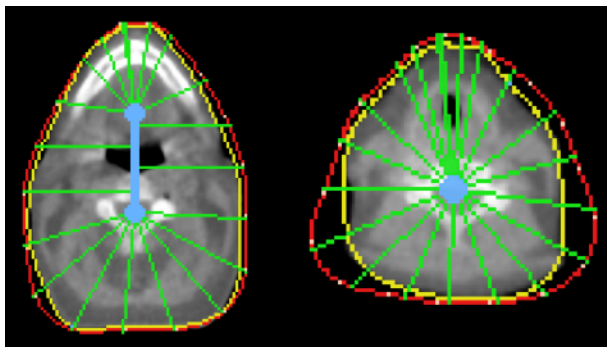


Figure 9: The difference between KV-CT skin (red contour) and MV-CT skin (yellow contour) is measured at 30 spline control points. Motion vectors (green) emanate outward from bone centroids (blue). Two different patients are depicted, where the case on the right experienced significantly more weight loss.

from the central axis to each of 30 control points. The control points form a spline that is fit to the boundary of the skin segmentation. The magnitude of the expansion is measured from the gap between the two splines representing KV-CT and MV-CT skin. The measured difference is distributed along the entire path from the centroid in accordance with the type of tissue present

along the path. In our computational model, fat tissue is favored to shrink 10:1 over muscle tissue. The sectors

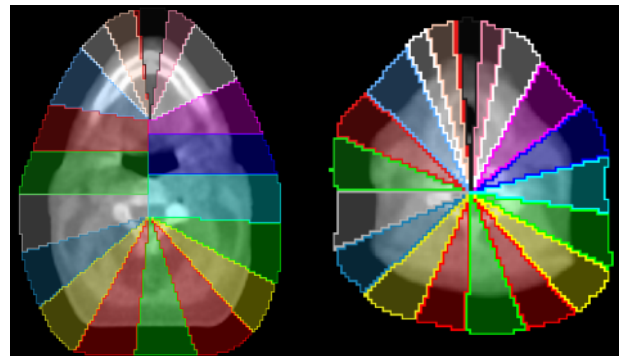


Figure 10: Sectors (colored uniquely) are defined to be the regions of the image corresponding to each control point. Voxels within each sector deform to a similar degree.

shown in Figure 10 facilitate robust measurements and assist in maintaining the effects to be smoothly varying. Figure 11 illustrates the results of varying the single parameter that is responsible for representing weight loss visible at the skin. Similarly, another parameter exists to control weight loss manifested at the pharynx.

Integrated Warp Field

Weight-loss deformation is computed after bone deformation, and added to the warp field with only the minimal smoothness required to maintain an invertible field, as shown in Figure 12. At each voxel, the impact of each actor is weighted by the distance to the actor's surface, as measured using euclidean distance transforms. The warp fields are intentionally carried outside the patient into the surrounding empty space, and then linearly ramped down gradually from there.

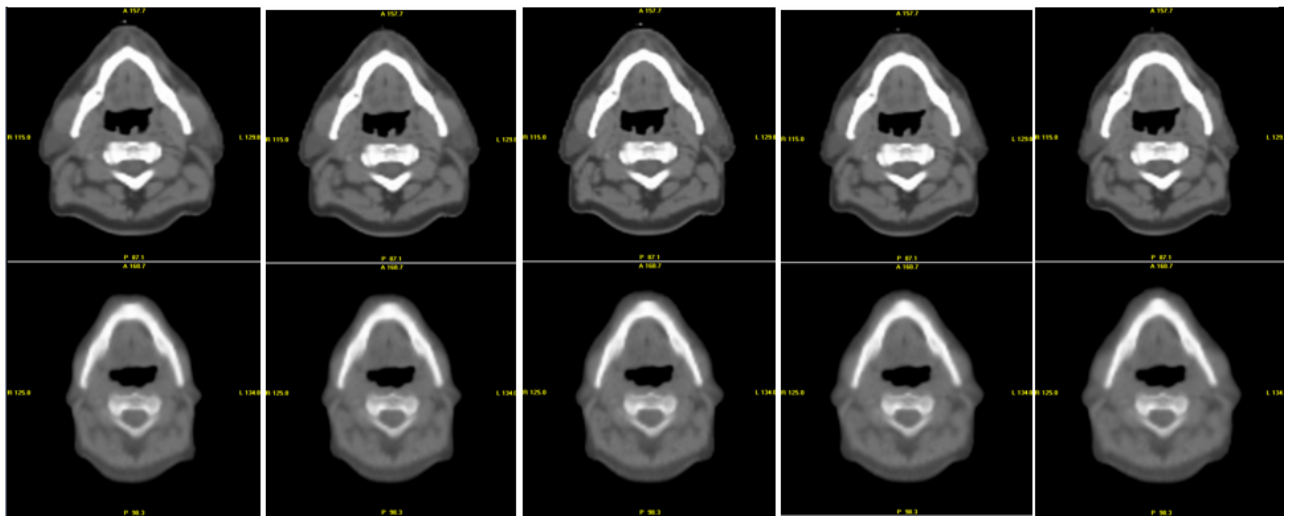


Figure 11: These images are generated by varying the single parameter governing weight loss. From left-to-right, weight is progressively “subtracted” from the KV-CT image along the top row, while being “added” to the MV-CT image below.

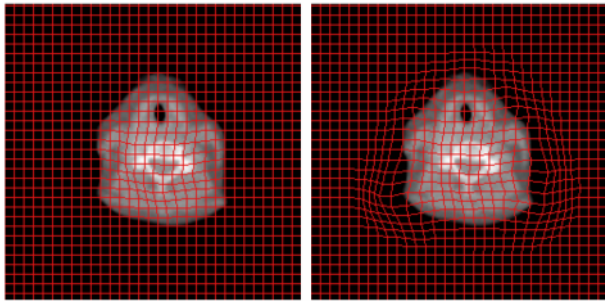


Figure 12: Left: warp field after processing bone alone. Right: field after skin and bone have both been processed.

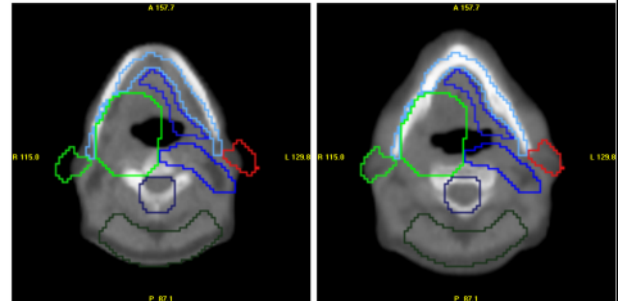


Figure 13: The MV-CT is shown with the planning contours overlaid. The result of rigid registration is on the left, while the result of ADD (not free-form) is on the right. Observe the significant motion of the mandible, and the change in patient weight.

Results and discussion

The segmentation and deformation method has been trained and tested on ten clinical head/neck datasets where the daily images are TomoTherapy® megavoltage CT scans. The average processing time, for volumes with roughly 110 slices and 256x256 pixels per slice, is only 40 seconds on a standard PC, without any human interaction.

Several types of errors that were evident when using free-from deformation were observed to be addressed by anatomically driven deformation (ADD). These included problems with distorted bones, the spinal cord leaving its cavity, muscle tissue leaking into nodal regions, and parotid gland issues near the periphery.

To obtain quantitative results, we compared the similarity measure computed after rigid registration, after ADD, and after free-from deformation. The percentage of the improvement in similarity captured by ADD was measured to vary between 52% and 82%.

To obtain qualitative results, we generated animations that warp the daily image to the planning image gradually by stepping along the deformation field. ADD

produced movies that are noticeably more visually pleasing, owing to the anatomic integrity of the recovered motion. Figure 13 presents sample frames.

Conclusion

Most of the changes observed across a course of treatment can be captured by a simple anatomical model. Using a model to initially constrain the deformation field can help mitigate deformation errors.

References

- [1] Gering D, Lu W, Ruchala K, Olivera G, 2008. An automatic contouring method that combines rule-based, atlas-based, and mesh-based approaches. *AAPM*.
- [2] Gering D, Lu W, Ruchala K, Olivera G, 2009. Utilizing shape models composed of geometric primitives for organ segmentation. *AAPM*.
- [3] Lu W, Ruchala K, Olivera G, 2004. Fast free-form deformable registration via calculus of variations. *Physics in Medicine*.

This work sponsored by TomoTherapy.